Diffusion Motions and Microphase Separation of Styrene–Butadiene Diblock Copolymer in Solution. 1. Extremely Dilute Solution Region

Yoshisuke Tsunashima,* Masukazu Hirata, and Yukinao Kawamata

Institute for Chemical Research, Kyoto University, Uji, Kyoto-fu 611, Japan.
Received March 30, 1989; Revised Manuscript Received August 8, 1989

ABSTRACT: Dynamical properties are investigated through dynamic light-scattering and viscometric measurements on a styrene (S)–butadiene (B) block copolymer ($M_w = 9.73 \times 10^4$, $M_w/M_n = 1.03 \pm 0.02$, 29.3 wt % PS) in dilute solutions of three good solvents, tetrahydrofuran (THF), benzene, and thiophenol, and in extremely dilute solutions of *n*-decane at 25 °C. Benzene is isorefractive to B subchains and thiophenol is isorefractive to S subchains, while *n*-decane is selectively good for B subchains but is precipitant for S subchains. In three good solvents, the SB copolymer is in molecular dispersion and takes a highly stretched conformation due to much stronger repulsive interactions between the same segments (S–S and B–B) than the interaction of the S–B segment. Intramolecular segregation of S and B subchains never occurs in this polymer/solvents system. In *n*-decane of polymer concentration c ranging from 1×10^{-6} to 5.7×10^{-4} g cm^{-3}, the SB copolymer shows conformational transitions depending on c. At $c < 3.8 \times 10^{-6}$ g cm^{-3} (region I), the SB chain disperses molecularly and the collapsed S-chain part, which is insoluble in *n*-decane, is covered with the soluble B-chain part of the same molecule. At highest c of $c > 1.1 \times 10^{-4}$ g cm^{-3} (region III) the SB chains coagulate intermolecularly and form micelles which are composed of the core of S chains and of the shell of surrounding B chains. These micelles are compact rigid spheres made of ca. 100 pieces of SB chains and disperse in solution in stable single micellar form. Moreover, in the intermediate concentration region of $3.8 \times 10^{-6} < c$ (g cm^{-3}) $< 1.1 \times 10^{-4}$ (region II) the SB chains construct huge but loosely packed micelles due to weak attractive interactions between intermolecular S chains of great numbers. Region II is considered to be in an unstable thermodynamical state and may be a transition region where the hard micelles become loose and decompose into the single molecular size.

I. Introduction

Block copolymers show in solution various types of conformational transitions, depending on manner in microphase separation. Microphase separation is affected strongly on the intra- and intersegment interactions, which change with solvent nature, polymer concentration, and temperature. Chemical structures and compositions of the polymer chains also control behavior of the transition. In the case of these polymer solutions, polymer molecules and solvents differ so much in dimension that the transitions take place generally at very low polymer concentrations. The investigations hitherto made have however little discussed the transitions in such extremely dilute concentration region as indicated above, though static (integrated) light-scattering measurements have provided fruitful aspects on conformational changes of block copolymers in "usual" dilute solution[1] and viscoelastic measurements have also given insight into three-dimensional structures of block copolymers in concentrated solution.[2] Moreover, the samples used there were diblock and triblock copolymers of various chain architecture. We consider that a single block copolymer of fixed-chain architecture gives information essentially enough to analyze the fundamental transitions occurring in block copolymers in dilute solution, and in this paper we take as a sample a styrene (S)–butadiene (B) diblock copolymer accordingly.

The SB diblock copolymer is of molecular weight $M_w = 9.73 \times 10^4$ ($M_w/M_n = 1.03 \pm 0.02$, 29.3 wt % PS). We investigate its conformational transitions in very dilute solutions in dynamical ways of dynamic light-scattering spectroscopy and of viscometry. First, dynamical and conformational properties of the SB copolymer are examined in three good solvents for both S and B subchains: tetrahydrofuran, benzene, and thiophenol, benzene being isorefractive to the B subchains and thiophenol being isorefractive to the S subchains. The polymers dissolve in these solvents molecularly. Second, dynamic characteristics are studied in *n*-decane, which is good and selective for B subchains but is precipitant for S subchains. Within the polymer concentration widely ranging from 10^{-4} to 10^{-6} g cm^{-3}, conformational transitions were detected, which can be distinguished from each other through particular molecular structures, i.e., a molecular dispersion (the S part is covered with the intramolecular B part) in extremely dilute solution and two types of associated micelles (the S parts are protected intermolecular B chains) in relatively dilute solution. These transitions are discussed in detail and are analyzed thermodynamically.

II. Experimental Section

A. Materials. A narrow molecular weight distribution diblock copolymer sample of styrene and butadiene (coded as SB1) was used, which was prepared by Prof. Kotaka's group of Osaka University under the living polymerization. The SB1 was dissolved in spectrograde benzene, the solution was then centrifuged twice to remove dust, and finally the supernatant liquid was collected in order to be submitted to freeze-drying. The weight-average molecular weight, M_w, of the purified SB1 was 9.73×10^4, and its styrene weight content was 0.293 (molar fraction 0.18). The M_w value was determined by a low-angle light-scattering photometer (LS-8, Tosoh) combined with a high-speed liquid chromatograph (HLC-802UR, Tosoh). The chromatograms obtained in this measurement with a SB1/THF solution are shown in Figure 1 in the plots of the refractive index increment, RI, and the scattered light-intensity, LS, against the elution volume. The SEC graphs guaranteed the sample to be monodisperse of $M_w/M_n = 1.03 \pm 0.02$. *n*-Decane was purified by fractionally distilling guaranteed grade *n*-decane (Nacalai Tesque, Kyoto) at 19 mmHg over $LiAlH_4$ under nitrogen atmosphere just prior to use. The boiling point of collected fractions was 69.0–69.5 °C at 19 mmHg, and the purity was about 100% as measured by gas chromatograph/mass spectroscopy. The refractive index of *n*-decane, n, for 488 nm was deter-

0024-9297/90/2223-1089$02.50/0

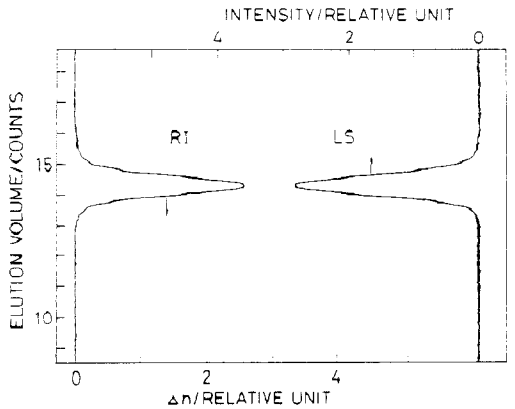

Figure 1. Chromatograms of a 1.056×10^{-3} g/g of solution of SB1 in THF at the flow speed of 1.1 cm^3/min. RI and LS in the abscissa represent the refractive index increment and the scattered-light intensity in relative units, respectively.

Table I
Optical Properties of Solvents and of Polystyrene (PS) and Polybutadiene (PB) Subchains of SB Diblock Copolymers for 488 nm at 25 °C

solvent	refractive index, n	dn/dc^a (±0.002) PS[b]	dn/dc^a (±0.002) PB[b]	solubility PS	solubility PB
benzene	1.5096	0.094	±0.00	good	good
THF	1.4091	0.194	0.132	good	good
thiophenol	1.6021	±0.00	−0.121	good	good
n-decane	1.4111	0.189	0.129	precipitant	good

[a] Calculated from the Grastone–Dale equation using the parameters determined by experimental dn/dc values.[18b] [b] Refractive indices of block subchains are 1.59–1.60[18c] and 1.516–1.526[18d] for PS and PB, respectively, for a sodium D line at 25 °C.

mined by interpolating to 488 nm the observed n values for Mercury (436-, 546-nm) lines and for a sodium D (589-nm) line on a Pulfrich refractometer at 25 °C. Tetrahydrofuran (THF) was obtained from Nacalai Tesque (Kyoto) as chromatographic grade THF and was used without further purification. The purity was checked by measuring its refractive index for Hg (436-, 546-nm) lines and for a Na-D line at 25 °C. The obtained value n_D^{25} = 1.404 66 agreed well with the literature value, 1.404 96.[3] Benzene was also obtained from the same company as spectrograde benzene. It was used without further purification since its purity was guaranteed through refractive index measurements made with the same procedure as described above. Thiophenol was purified by fractionally distilling reagent-grade thiophenol (Nakarai Tesque) under nitrogen atmosphere at 48 °C (7 mmHg). The distilled solvent was sealed in test tubes under nitrogen atmosphere until it was used for preparation of solutions. The refractive index measurement guaranteed the purity of thiophenol. The result on these solvents for 488 nm at 25 °C was summarized in Table I. The solvent viscosity (×10^{-2} g cm^{-1} s^{-1}) was 0.6028 (benzene), 0.8543 (n-decane), 1.187 (thiophenol), and 0.4600 (THF).

B. Preparation of Sample Solutions. Dilute solutions of SB1 in benzene, thiophenol, and THF with different polymer concentration were made, in a nitrogen-filled drybox, by directly filtering pure solvent and an original polymer solution into dust-free DLS cells through a Millipore filter (0.22-μm pore size). The original solutions were prepared, prior to filtration, by sealing weighed amounts of the freeze-dried SB1 and the solvent in a dust-free test tube under N_2 atmosphere and then by heating the sealed tube at ca. 40 °C for 24 h with intermittent shaking. Dilute solutions of SB1 in n-decane were prepared carefully because n-decane was a precipitant for S subchains. SB1 and n-decane were sealed in a tube as described above and then heated at ca. 50 °C for a few days until a homogeneous clear solution appeared, during which time the solution changed color from opaque milk white to clear light opalescent. After this treatment, the solution remained with its scattering intensity unchanged. The original solution thus prepared was next filtered through a Millipore filter (0.45-μm pore size) into dust-free DLS cells where the desirable amount of n-decane was put in advance through a 0.22-μm Millipore filter. Finally, the mixed solutions were heated again overnight at 50 °C.

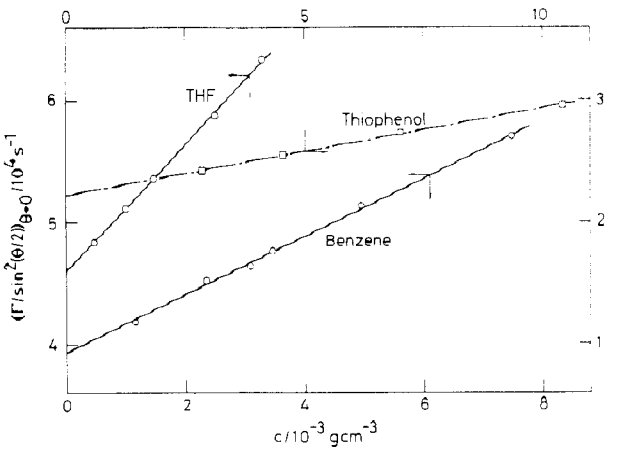

Figure 2. First cumulants $\Gamma_{q\to 0}(c)$ for SB1 in good solvents at 25 °C are plotted in the form of $\Gamma_{q\to 0}(c)/\sin^2(\theta/2)$ against polymer concentration c.

C. Methods. The normalized autocorrelation function of the scattered light intensity was measured on our laboratory-made 512-channel time-interval correlator[4] with a Spectra-Physics 3-W argon ion laser (Model 2020-30/2560), an etalon being equipped to ensure the single frequency of the 488-nm line. The vertically polarized scattered-light component due to the vertically polarized incident light, V_v, was accumulated for at least 1 h to make sure all the data points were within 2–3% of fluctuation and to ascertain the base line to be 1.000 ± 0.003. Scattering angles used were 10°, 30°, 60°, 90°, 120°, and 150°. The correlation function measured was analyzed with a weighted nonlinear least-squares algorithm on a FACOM M-380Q computer in our institute. The solution viscosity was measured with a Cannon-Fenske type of four-bulb spiral capillary viscometer[5] and with a usual Ubbelohde capillary viscometer. Using two types of viscometers, we could change the shear rate in solution from 40 to 2800 s^{-1}. All the measurements made in the present work were pursued at 25.00 ± 0.02 °C.

III. Results

A. SB1/THF, SB1/Benzene, and SB1/Thiophenol Solutions. The autocorrelation functions were measured at scattering angles $\theta \leq 90°$ and at polymer concentrations $c < 1 \times 10^{-2}$ g cm^{-3}. All the functions measured showed single-exponential type decays and gave the decay rates $\Gamma(q,c)$ as a function of θ and c. Here q is the magnitude of the scattering vector, $|\mathbf{q}| = (4\pi n/\lambda_0) \sin(\theta/2)$, with n the refractive index of solvent and λ_0 the wavelength of the incident light in vacuo. Extrapolating $\Gamma(q,c)$ to $q = 0$, we determined the first cumulant $\Gamma_{q\to 0}(c)$ at finite c, where $\Gamma_{q\to 0} = D(c)q^2$ with $D(c)$ the translational diffusion coefficient at finite polymer concentration. Figure 2 shows plots of $\Gamma_{q\to 0}(c)/\sin^2(\theta/2)$ versus c for SB1 in THF, benzene, and thiophenol. The data points were represented well by the equations linear to c

$$D(c) = D_0(1 + k_D c) \quad (1)$$

and yielded the translational diffusion coefficient at infinite dilution, D_0, and the concentration coefficient, k_D. Using the Stokes–Einstein equation

$$D_0 = k_B T/6\pi\eta_0 R_H \quad (2)$$

we estimated the hydrodynamic (Stokes) radius, R_H. Here k_B denotes the Boltzmann constant and η_0 the solvent viscosity. Table II summarizes the experimental values of D_0, k_D, and R_H thus obtained.

Table II
Dynamic Characteristics of Styrene–Butadiene Diblock Copolymer SB1 in THF, Benzene, and Thiophenol at 25 °C[a]

solvent	$10^8 D_0$, cm^2 s^{-1}	k_D, cm^3 g^{-1}	R_H, nm	$[\eta]$, cm^3 g^{-1}	k'	R_V, nm	R_V/R_H	β_{FSM}, 10^6
THF	34.9	114	13.8	98.6[b]	0.42[b]	11.5	0.833	1.760
benzene	26.0	60.5	13.9	94.0[c]	0.38[c]	11.3	0.813	1.717
thiophenol	13.0	31.9	14.1					

[a] The values $D_0 = 87.2 \times 10^{-8}$ cm^2 s^{-1} and $R_H = 4.5$ nm should be referred for PS homopolymers in benzene of the same molecular weight as the S part of SB1. [b] Measured under the shear rate $G = 2800$ s^{-1}. [c] Measured under the shear rate $G = 2100$ s^{-1}.

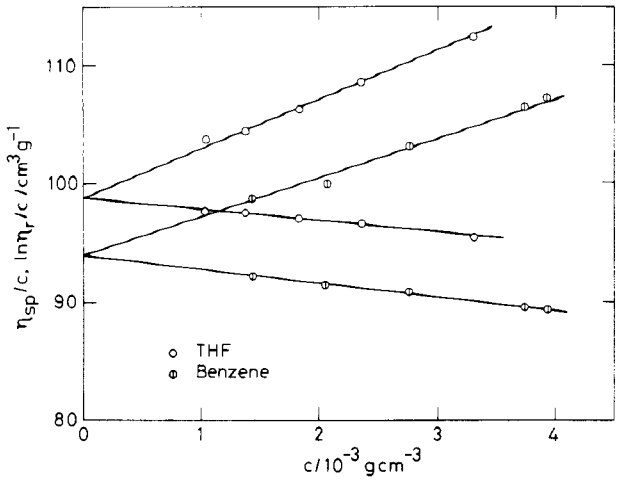

Figure 3. Concentration dependences of the solution viscosity for SB1 in good solvents at 25 °C. The shear rate was 2800 and 2100 s^{-1} in THF and benzene, respectively.

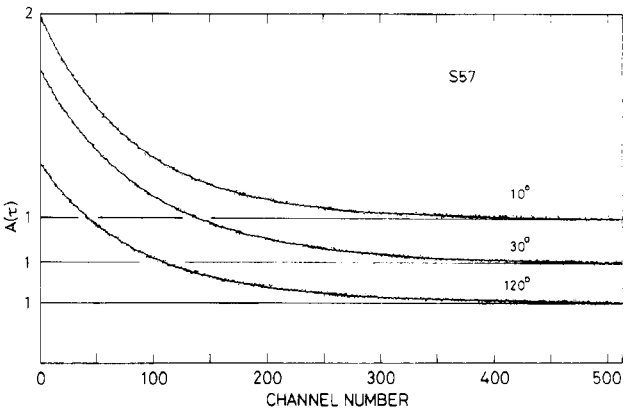

Figure 4. Normalized autocorrelation functions $A(\tau)$ measured at $\theta = 10°$, 30°, and 120° for the dilute SB1/*n*-decane solution S57 of polymer concentration $c = 56.9_3 \times 10^{-5}$ g cm^{-3} at 25 °C. The dots represent data points, and the solid lines represent the data-fitted single-exponential decay curves. $A(\tau)$ at $\theta = 30°$ and 120° is shifted downward, respectively, by the amount indicated with each base line at $A(\tau) = 1.000$. Channel numbers on the abscissa i represent the correlation time, τ, with the relation that $\tau = i\Delta\tau$. Here $\Delta\tau$ means the delay time in each channel and is 100, 10, and 1 μs at $\theta = 10°$, 30°, and 120°, respectively.

Figure 3 shows concentration dependences of solution viscosity for SB1 in THF and benzene. In this figure, the viscosity data in both solutions are plotted according to the Huggins equation,[6] $\eta_{sp}/c = [\eta] + k'[\eta]^2 c$, and to the Mead–Fuoss equation,[6] $\ln \eta_r/c = [\eta] - \beta[\eta]^2 c$, with η_{sp} the specific viscosity, η_r the relative viscosity, k' the Huggins constant, and $\beta = 0.5 - k'$. The intercepts at $c = 0$ and the slopes gave the intrinsic viscosity, $[\eta]$, and k' as listed in Table II.

B. SB1/*n*-Decane Solutions. The autocorrelation functions were measured at $\theta = 10° - 150°$ for nine solutions of concentration ranging from 5.69×10^{-4} to 1.04×10^{-6} g cm^{-3}, as are summarized in Table III. We coded these solutions as S*ff*, where *ff* represents the value of polymer concentration expressed in 10^{-5} g cm^{-3} units: S0.9, for example, denotes the solution of $c = 0.955 \times 10^{-5}$ g cm^{-3}. The measured functions were all single-exponential type decay curves as is typically illustrated in Figures 4–6 for three solutions of different orders in concentration magnitude; S57, S4, and S0.4. Here only three curves are illustrated at $\theta = 10°$, 30°, and 120°. The frequency, which is the magnitude of the correlation function at $\tau = 0$, decreases drastically from ca. 0.9 for S57 and S4 to ca. 0.2 for S0.4 at $\theta = 30°$. The decay rate $\Gamma(q,c)$ was estimated for each curve using the same procedure mentioned before. It should be noticed that we observe *monodisperse* particles whatever the particle conformations are, because the autocorrelation function, in any case we examined, was characterized by its single-exponential decay, which is clearly exhibited with such a small value of the normalized second moment (the variance) μ_2/Γ^2 as is tabulated in the last column of Table III, and because the autocorrelation function left no trace of bimodal decay when the function was analyzed through a histogram method,[7] which can distinguish the presence of a bimodal distribution of the decay rate even if $\mu_2/\Gamma^2 \simeq 0.08$.

Figure 7 shows plots of $\Gamma(q,c)/\sin^2(\theta/2)$ versus $\sin^2(\theta/2)$ for six relatively higher concentration solutions, S57–S0.4. The other three lower concentration solutions, F1.1, S0.3, and S0.1, we will describe later. Figure 7 reveals that $\Gamma(q,c)$ has q^2 dependence in this c region for each solution. We therefore estimated from the $\Gamma(q=0,c)$ values the diffusion coefficients $D(c)$ and listed them in Table III. They are plotted against c in Figure 8. Only four points, except the higher two, show the linear concentration dependence, of which simple linear extrapolation to $c = 0$ (solid line) gives the result that $D_0(\text{II}) = 4.49 \times 10^{-8}$ cm^2 s^{-1} ($R_H(\text{II}) = 56.8$ nm) and $k_D(\text{II}) = 2450$ cm^3 g^{-1}. Here II means the concentration region II where dynamical properties differ from those in other regions that will be referred to later. Contrarily, the higher two points in the figure are never located on the extension of the solid line shown there. Rather they are on another line (broken line) of which the $D(c)$ versus c relation will yield smaller k_D and larger D_0 values, if these data were expressed by eq 1. We call this region III. We will discuss later in detail the differentiation made between regions II and III.

For lowest concentration solutions S0.3 and S0.1, the scattered light intensity was about half of that for S0.4 and the correlation functions were available only at $\theta = 10°$. Figure 9 reveals this situation well, where the case of S0.1 at $\theta = 10°$ is illustrated. The correlation functions measured in this region gave $D(c)$ values 10 times larger than those of region II, as are listed in Table III. We call this extremely low concentration region I accordingly. The same situation was observed for solution F1.1. This solution was prepared so as to exclude possible SB micellar formation in a solution (S1.1) of concentration 1.07×10^{-5} g cm^{-3}: S1.1, which was prepared according to the procedure described already, was filtered again through a 0.1-μm Millipore filter, and then heated over-

Table III
Dynamic Characteristics of Styrene–Butadiene Diblock Copolymer SB1 in *n*-Decane of Low Concentrations at 25 °C

solution code	concn, c, 10^{-5} g cm^{-3}	$10^8 D(c)$, cm^2 s^{-1}	$R_H(c)$,[a] nm	$[\eta]$, cm^3 g^{-1}	k'	region (c_i, 10^{-5} g cm^{-3})	$10^8 D_0$,[b] cm^2 s^{-1}	k_D,[b] cm^3 g^{-1}	μ_2/Γ^2
S57	56.9_3	5.97	42.8			III			0.019
S21	20.7_6	5.90	43.3						0.016
	$(c \to 0)$[b]		43.5[b,c]	53.5[b]	1.42[b]		5.9[c]	35[c]	
						($c_2 \simeq 11$)			
S7	7.59_0	5.36	47.7						0.022
S4	3.84_8	4.86	52.5						0.010
S0.9	0.955_0	4.60	55.5			II			0.008
S0.4	0.469_2	4.58	55.8						0.022
	$(c \to 0)$[b]		56.8[b]				4.49	2450	
						($c_1 \simeq 0.38$)			
F1.1[d]	<1.070	47.9	5.3						0.056
S0.3	0.310_0	50.2	5.1			I			0.040
S0.1	0.104_1	55.3	4.6						0.041
	$(c \to 0)$[b]		4.7[b]				54.3	...	

[a] $R_H(c)$ was estimated by assuming that the Einstein–Stokes equation holds in dilute but finite polymer concentration; $D(c) = k_B T/6\pi\eta_0 R_H(c)$. [b] Values extrapolated simply to infinite dilution. See the text and ref 21. [c] Reference 20. [d] The solution was filtered through a 0.10-μm Millipore filter.

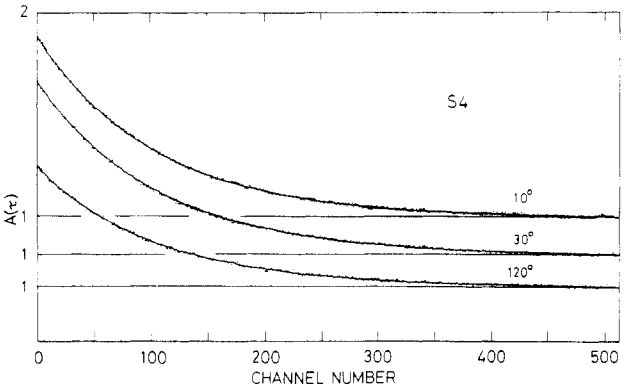

Figure 5. $A(\tau)$ measured at θ = 10°, 30°, and 120° for the dilute SB1/*n*-decane solution S4 of $c = 3.84_8 \times 10^{-5}$ g cm^{-3} at 25 °C. $\Delta\tau$ was 100, 10, and 1 μs at θ = 10°, 30°, and 120°, respectively. The ordinate and the abscissa are treated in the same manner as in Figure 4.

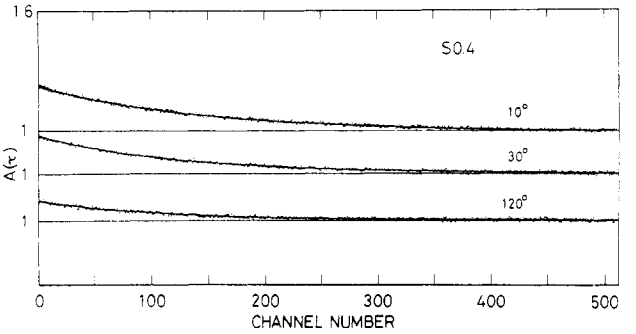

Figure 6. $A(\tau)$ measured at θ = 10°, 30°, and 120° for the very dilute SB1/*n*-decane solution S0.4 of $c = 4.69_2 \times 10^{-6}$ g cm^{-3} at 25 °C. $\Delta\tau$ was 100, 10, and 1 μs at θ = 10°, 30°, and 120°, respectively. The ordinate and the abscissa are treated in the same manner as in Figure 4.

night at 50 °C.[8] The result for F1.1 is also listed in Table III.

Next, we measured the solution viscosity to examine a possibility that strong shear rate breaks SB micelles, if formed, into more stable small particles. Figure 10 shows the solution viscosity measured by a Ubbelohde viscometer (G = 1250 s^{-1}) as a function of c, where the concentration was higher than 1×10^{-3} g cm^{-3}. Plots of η_{sp}/c versus c (line 1) and of ln η_r/c versus c (line 2) gave that $[\eta]$ = 53.5 cm^3 g^{-1} and k' = 1.42. For lower concentration solutions of c such as $1 < 10^4 c$ (g cm^{-3}) < 13, which corresponds to region III, we used a spiral capillary viscometer and obtained the result exhibited in Figure 11. Here the data are plotted in the form of η_{sp}/c versus c, and the solution shear rates were 40, 70, and 100 s^{-1}. Independent of the shear rate, data points are all located closely on the straight line, which represents exactly the same line (line 1) that is drawn in Figure 10 on data at $c > 1 \times 10^{-3}$ g cm^{-1}. The $[\eta]$ and k' values obtained above characterize the viscosity behavior of SB1 in region III as a result. They are listed in Table III. Experiments at $c < 1 \times 10^{-4}$ g cm^{-3} (region II) are beyond the ability of viscosity measurements, and consequently, the viscometric behavior in this region is left open to question.

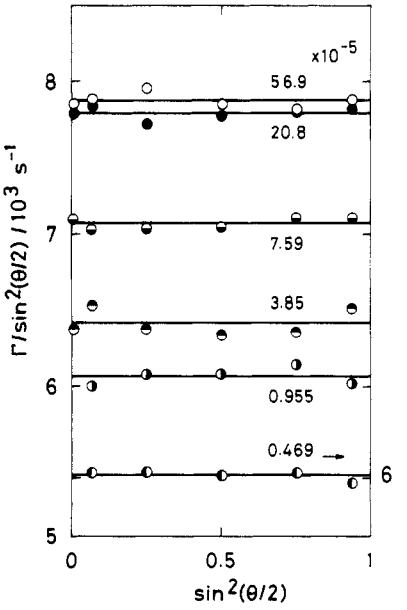

Figure 7. Scattering angle (θ) dependences of the first cumulants Γ measured for SB1 in *n*-decane in the dilute to very dilute polymer concentration regions at 25 °C. The numbers attached on each line represent magnitudes of the solution concentration.

IV. Discussion

A. Properties in Good Solvents. Subchains B of SB1 are isorefractive to benzene. In very dilute solution, the autocorrelation function for SB1 in this solvent reflects only the scattered light intensity due to the intramolecular S chain since SB1 disperses molecularly. The D_0 or R_H value in this case gives the intramolecular hydrodynamic dimension of the S chain[9] and will differ from the dimension value of homopolymer S chains of

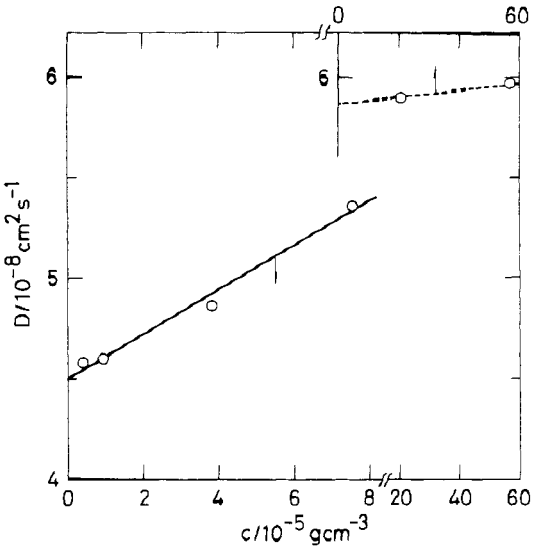

Figure 8. Concentration dependences of the diffusion coefficients, $D(c)$, measured for SB1/*n*-decane solutions in the dilute to very dilute polymer concentration regions. The data points in two classified concentration regions are simply extrapolated to $c \rightarrow 0$ as is represented by the solid and the broken lines, respectively.

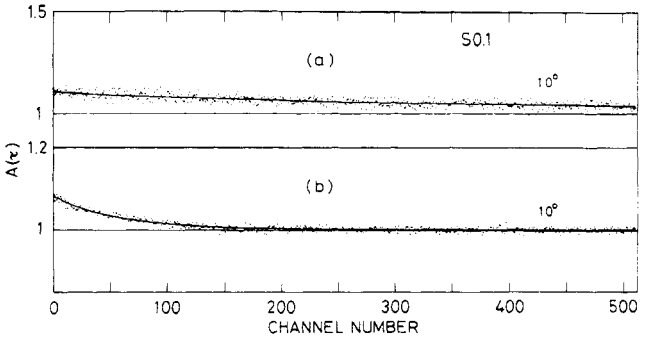

Figure 9. Normalized autocorrelation functions $A(\tau)$ measured at $\theta = 10°$ for the extremely dilute SB1/*n*-decane solution S0.1 of $c = 1.04_1 \times 10^{-6}$ g cm^{-3}: the delay time, (a) $\Delta\tau = 1$ μs; (b) $\Delta\tau = 15$ μs. The ordinate on (b) is enlarged to 2 times larger than that of (a) and of Figures 4–6.

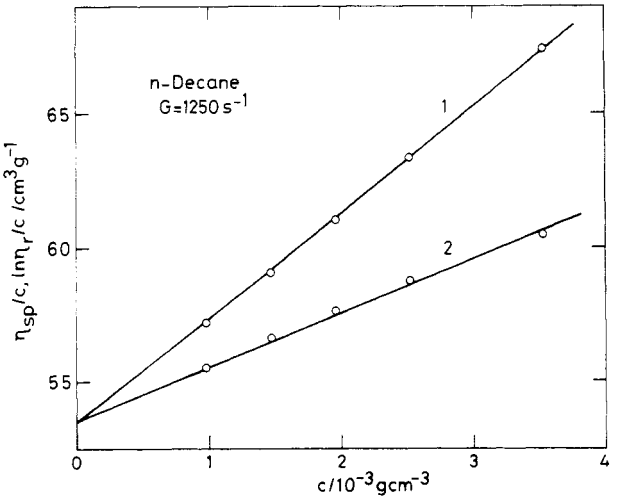

Figure 10. Huggins (line 1) and Mead–Fuoss (line 2) plots of the solution viscosity measured for dilute SB1 solutions in *n*-decane at 25 °C. The shear rate was 1250 s^{-1}.

the same molecular weight, $R_{H,homo}$. The difference depends on the magnitude of the interactions between S–S segments, B–B segments, and S–B segments of the SB molecule in benzene. Substituting the molecular weight

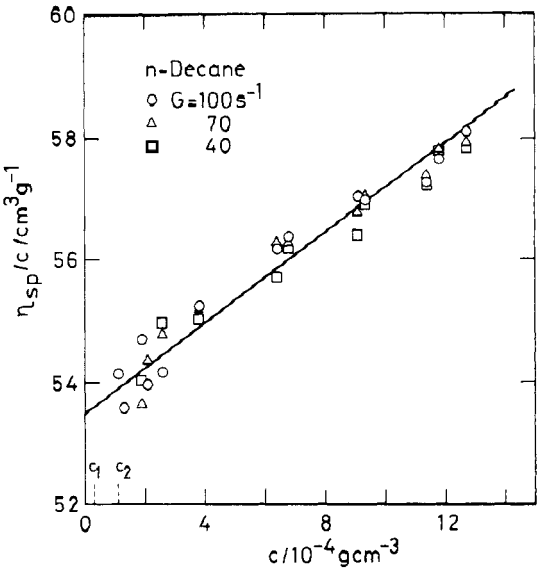

Figure 11. Huggins plots of the solution viscosity measured for very dilute SB1/*n*-decane solutions at 25 °C. Three different shear rates 100, 70, and 40 s^{-1} were applied to the solutions. c_1 and c_2 denote the crossover concentrations, which are discussed in the text.

of the S part $0.293(9.73 \times 10^4)$ into our previous empirical relation for homopolymer PS in benzene at 25 °C, $R_H = 1.60 \times 10^{-9} M_w^{0.55}$ (cm),[10] we can estimate the $R_{H,homo}$ value as $R_{H,homo} = 4.5$ nm, which is about one-third of the experimental one, $R_H = 13.9$ nm (Table II). $R_{H,homo}$ could never exceed 8.9 nm even if the SB1 molecule were entirely replaced by PS of the same molecular weight. These facts indicate that (a) the intramolecular separation does not occur in the S and B subchains and that (b) the S and B chains interpenetrate each other in a highly stretched state as compared with the states they have in the case of the homopolymers. In thiophenol where only B subchains are visible optically, SB1 shows exactly the same R_H value, 14.1 nm (Table II), as that in benzene. In THF where S and B chains are both visible optically, the SB1 gives that $R_H = 13.8$ nm, in good agreement with R_H in benzene. Thus, the R_H values confirm that both S and B parts of single SB1 molecule expand to a great extent in good solvents. The concentration coefficient, k_D, is a measure of polymer–polymer interactions and is proportional to the second virial coefficient multiplied by molecular weight, $A_2 M_w$, in good solvent limit.[11] The values $k_D = 114$ cm^3 g^{-1} in THF and 60.5 cm^3 g^{-1} in benzene are surprisingly large when compared with the value $k_{D,homo} = 28$ cm^3 g^{-1}, which is predicted for PS of the same molecular weight as SB1 in benzene.[11] This suggests that there is strong repulsive interaction between *intermolecular* S–S, B–B, and/or S–B segments.

As shown in Table II, the value of $[\eta]$ in THF is nearly equal to that in benzene and is also the case for k'. If we assume that polymer chains in good solvents could be modeled by hard spheres of radius R_V, we can calculate the viscometric radius as

$$R_V = [(3/4\pi)(2/5N_A)]^{1/3}(M_w[\eta])^{1/3} = 5.413 \times 10^{-9}(M_w[\eta])^{1/3} \text{ (cm)} \quad (3)$$

The calculated values are 11.3–11.5 nm (Table II) and are equal to each other in both solvents, being comparable with R_H in both solvents. It is of interest to note that the obtained R_V/R_H ratios 0.81–0.83 are smaller than the values reported experimentally for flexible linear

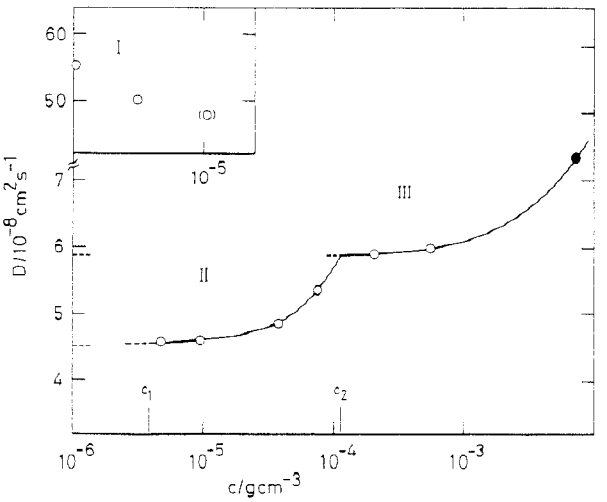

Figure 12. Concentration-dependent transition phenomena of the translational diffusion coefficients, D, for SB1 in n-decane at 25 °C. The concentration regions I–III are referred to in the text. The filled circle at the highest concentration ($c = 7.24 \times 10^{-3}$ g cm^{-3}) is a typical example of the data that will be shown in the forthcoming paper.[20] This will make clear a strong connection between the present data for S21 and S57 and the filled data in region III.

homopolymers in good solvents, 0.97–1.14,[5,12,13] and smaller than the theoretical value for rigid spheres 1.00. More strictly speaking, this ratio can be discussed in terms of a universal ratio, β_{FSM}, which was introduced by Mandelkern, Flory, and Scheraga[23] with the definition that $\beta_{FSM} = (M[\eta]/100)^{1/3}(D_0\eta_0/k_BT)$. The β_{FSM} values of $(1.72–1.76) \times 10^6$ for the SB chains are smaller than both values of 2.11×10^6 and 2.19×10^6 for rigid spheres[14] and flexible homopolymers in good solvents,[15] respectively. For prolate ellipsoids with the axes a, b, and b, the value β_{FSM} increases with an increase in the axial ratio, p ($=a/b$): 2.11×10^6 at $p = 1$ (spheres) and 2.68×10^6 at $p = 20$ (rodlike particles).[14] The small β_{FSM} values for the SB chains are left open to question. On the other hand, the experimental value $k' \simeq 0.4$ is very close to a theoretical good solvent limit value 1/3 for flexible homopolymer chains.

According to the Kurata–Kimura theory[16] of AB diblock copolymers in dilute solution, it is predicted that, in good solvents for both A and B subchains, (i) AB diblock chains expand much more than homopolymer chains do and (ii) the sum rule holds for $[\eta]$, $[\eta] = [\eta]_A + [\eta]_B$, if repulsive intrasegmental interactions work between not only the same segments A–A and B–B but also the different segments A–B and if the former is much stronger than the latter. It should be noticed that the sum rule, which holds in *nonselective* solvents, never results from the intramolecular phase separation (segregation), which is caused by the repulsive A–B interaction.[17] The observed high extension of SB1 chains is therefore qualitatively explainable through the predominant repulsive interactions in S–S and B–B intrasegments over the S–B segment interaction. Quantitative comparison between experiments and the Kurata–Kimura theory can be achieved through the following result: with the estimated values $[\eta]_B \simeq 97$[18a] and $[\eta]_S \simeq 19$,[18a] we predicted that $[\eta] \simeq 116$ cm^3 g^{-1}, which is compared to within 18% with the experimental one, 98.6 cm^3 g^{-1}, in THF.

B. Properties in Selective Solvent. Dynamic light-scattering data in n-decane indicate that the SB1 molecules take concentration-dependent conformational transitions in the selective solvent. Figure 12 makes this clear, where nine $D(c)$ values obtained[19] are plotted against the logarithmic polymer concentration, c. These data points can be classified into three groups, I–III, from lower to higher concentration, as coded before, at which group boundaries the concentration dependence of $D(c)$ becomes discontinuous in its curve. We denote these two crossover concentrations as c_1 and c_2 with the roughly estimated values $c_1 \simeq 3.8 \times 10^{-6}$ and $c_2 \simeq 1.1 \times 10^{-4}$ g cm^{-3}. In region I, $D(c)$ increases with decreasing c and gives that $D_0(I) = 54 \times 10^{-8}$ cm^2 s^{-1} ($R_H(I) = 4.7$ nm). We, however, regard that the $D(c)$ is roughly constant, independent of c, with the average value $D_0(I) = 51 \times 10^{-8}$ cm^2 s^{-1} ($R_H(I) = 5.0$ nm) in view of the experimental ambiguity induced from low-frequency autocorrelation functions (e.g., Figure 9). This $D_0(I)$ value has the same order of magnitude as that in good solvents. The R_H value 5.0 nm is about one-third of that for SB1 in good solvents and is very close to the PS value in benzene of molecular weight, exactly the same as that of S subchains, 4.5 nm. We conclude as a result that SB diblock chains disperse monomolecularly in region I and that in the chains the B part swells well and protects the collapsed S part intramolecularly.

In region III, i.e., in the highest concentration region at $c > c_2$, the $\Gamma(q,c)/q^2$ values are constant and independent of q (Figure 7), though the result of only two polymer solutions, S57 and S21, was shown in the present paper. (The data of higher polymer concentration than S57 will be presented in the forthcoming paper,[20] where the $D(c)$ values for S21 and S57 are represented by a $D(c)$ vs c relation completely different from that in region II. Appearance of new modes other than translations will also be referred to there.[24] One data of the filled circle at $c = 7.24 \times 10^{-3}$ g cm^{-3} in Figure 12 is a typical illustration of those data that were obtained at concentrations, in region III, much higher than those in the present paper.[24]) The constancy of Γ/q^2 against q^2, mentioned above, means that we observe a translational diffusion process of the particles, which disperse in solution with uniform size. The two $D(c)$ data, moreover, make us expect that this process could be characterized through the values of $D_0(III) \simeq 5.9 \times 10^{-8}$ cm^2 s^{-1} and $k_D(III) \simeq 35$ cm^3 g^{-1} if we assume that the data in this region could be simply extrapolated to infinite dilution with the relation

$$D(III) = D_0(III)[1 + k_D(III)c] \quad (4)$$

Here $D_0(III)$ is defined only in region III as

$$D_0(III) = \lim_{c\to 0} D(III) \qquad R_H(III) = k_BT/6\pi\eta_0D_0(III) \quad (5)$$

The $D_0(III)$ and $k_D(III)$ values will be made sure in the forthcoming paper[20] using much higher concentration solutions of $7 \times 10^{-4} < c$ (g cm^{-3}) $< 1 \times 10^{-2}$. These values are ca. 1/10 and 1/3–1/2 of those in good solvents, respectively. The small $D_0(III)$ but comparable $k_D(III)$ values indicate that SB diblock copolymers construct compact micelles: S parts associate intermolecularly and collapse to a dense form (core), while B parts swell and cover the core, forming the outer shell. As is clearly shown in Figures 10 and 11, the SB molecules are viscometrically stable in conformation and are never affected by the shear rate of 40–1250 s^{-1}. Its conformation is characterized by the limiting values $[\eta] = 53.5$ cm^3 g^{-1} and $k' = 1.42$.[21] This $[\eta]$ value is only half that of good solvent ones, while k' is extremely large and is compared well with the theoretical value $k' = 2$ for rigid spheres but not with $k' = 1/3$ for flexible chains in good solvents and with 1/2 for those in θ solvents. This fact shows that the associated micelles have a hard-sphere structure whose inside is compactly packed with lots of chains. Equation 3 gives the

relation between $[\eta]$ and the radius R for hard-sphere molecules. Substituting the values $[\eta] = 53.5$ cm^3 g^{-1} and $R_H = 43.5$ nm, which was determined from D_0(III) $= 5.9 \times 10^{-8}$ cm^3 s^{-1}, into eq 3, we obtain the molecular weight of the micelle as 9.7×10^6. Since the molecular weight of single copolymer SB1 is 9.73×10^4, the micellar particle is constructed from 100 pieces of the copolymers.

In region II where $c_1 < c < c_2$, the values of $\Gamma(q,c)/q^2$ are independent of q^2 at every c, as is shown by lower four solid lines in Figure 7. Consequently, we notice that there is a translational diffusion process due to the particle of another type of molecular conformation. The characteristic values[21] are that R_H(II) = 56.8 nm (D_0(II) $= 4.49 \times 10^{-8}$ cm^2 s^{-1}) and k_D(II) = 2450 cm^3 g^{-1}. The former is 30% larger in magnitude than that of collapsed micelles and the latter is enormously large when compared with k_D of collapsed micelles and of single SB molecules in good solvents. This fact indicates that there is a micellar formation of a huge size in region II. The particle–particle interaction term k_D, which is proportional to A_2M in good solvent limit (hard-spherical interactions), is so large that we could imagine that the particle may be composed of enormous amounts of copolymers which connect loosely through much weaker intermolecular attraction between the S parts than is the case of the hard micelles in region III.

Kimura and Kurata[22] have developed a mean-field theory of A_2 and the third virial coefficient, A_3, for block copolymers in solution and found that A_2 and A_3 are positive at small c but A_3 changes, prior to A_2, from positive to negative as c increases in dilute *diblock* copolymer solutions of selective solvents. (A case of $A_2 < 0$ and $A_3 > 0$ seldom occurs, where the solution separates into dilute and concentrated phases in a certain region of c.) In this case, the osmotic pressure of solution, Π, expressed in power series of c as

$$\Pi/RT = c/M + A_2c^2 + A_3c^3 + \dots \quad (6)$$

exhibits only a maximum at a certain concentration, c_M, and afterward it decreases without limit with increasing c, making the solution unstable (appearance of precipitation). Region I thus corresponds to the state at small c where $A_2 > 0$ and $A_3 > 0$. We can discuss regions II and III as follows. We have the relation that $k_D = 0.36A_2M$ for hard-spherical interactions[11] with M the molecular weight of the sphere. The positive k_D in regions II and III indicates positive A_2 in both regions accordingly. The sign of A_3 is indefinite because $D(c)$ was linearly proportional to c in the measured c range in both regions II and III, as is shown in Figure 8. The positive A_2 is in qualitative agreement with the Kimura–Kurata theory for diblock copolymer solutions, indicating that regions II and III correspond to the states which will be realized in a polymer concentration region limited between small c and around or over c_M.

Finally, it is noted that the experimental values of micellar radii obtained here would allow more quantitative comparison with several theoretical works on micelles in selective solvents[25,26] if the interaction parameters would be made clear concerning block subchains and solvent in the present system.

In conclusion, we examined dynamical properties of a styrene–butadiene (SB) diblock copolymer in dilute solutions of three good solvents, THF, benzene, and thiophenol, and of a selective solvent, *n*-decane, and obtained the following results: In good solvents, the S and B parts of the copolymer extend a great deal longer than they are in the cases of the homopolymers of the same molecular weight. This chain conformation is due much more to the stronger repulsive interactions between the same segments S–S and B–B than to the S–B segment interaction. The intramolecular segregation does not occur in these solvents. In *n*-decane, the SB copolymer takes three types of molecular conformation, depending on the polymer concentration, c. The copolymer disperses molecularly in such extremely dilute solutions as c less than 3.8×10^{-6} g cm^{-3}, while in the range of c as $3.8 \times 10^{-6} < c$ (g cm^{-3}) $< 1.1 \times 10^{-4}$ it forms huge but loosely packed micelles due to weak attractive interactions between intermolecular S chains of great numbers. At higher c as $c > 1.1 \times 10^{-4}$ g cm^{-3}, the S parts of the copolymers collapse intermolecularly and construct the core of the hard-sphere type of micelles where ca. 100 pieces of copolymers coagulate very compactly. It is interesting to note that, in both cases where the micellar formation occurs, the micelles disperse homogeneously in solution with uniform size.

Acknowledgment. The sample SB1 is a gift from Professor T. Kotaka and Dr. H. Watanabe of Osaka University; this is acknowledged gratefully.

References and Notes

(1) For example: Utiyama, H.; Takenaka, K.; Mizumori, M.; Tsunashima, Y.; Kurata, M. *Macromolecules* **1974**, *7*, 515. Utiyama, H.; Takenaka, K.; Fukuda, M. *Ibid.* **1974**, *7*, 28. Tanaka, T.; Kotaka, T.; Inagaki, H. *Polym. J.* **1972**, *3*, 338 and the references cited in their series.
(2) For example: Kotaka, T.; Watanabe, H. *J. Soc. Rheol., Jpn.* **1982**, *10*, 24.
(3) Riddick, J. A.; Bunger, W. B. *Organic Solvents*, 3rd ed.; Wiley-Interscience: New York, 1970.
(4) Nemoto, N.; Tsunashima, Y.; Kurata, M. *Polym. J.* **1981**, *13*, 827.
(5) Tsunashima, Y.; Hirata, M.; Nemoto, N.; Kurata, M. *Macromolecules* **1988**, *21*, 1107.
(6) Huggins, M. L. *J. Am. Chem. Soc.* **1942**, *64*, 2712. Mead, D. F.; Fuoss, R. M. *Ibid.* **1942**, *64*, 277.
(7) Gulari, E.; Gulari, E.; Tsunashima, Y.; Chu, B. *J. Chem. Phys.* **1979**, *70*, 3966. Tsunashima, Y.; Nemoto, N.; Kurata, M. *Bull. Inst. Chem. Res., Kyoto Univ.* **1981**, *59*, 293.
(8) Since SB1 particles have the size of $2R_H = 114$ nm at $c = 1.07 \times 10^{-5}$ g cm^{-3} (region II), this filtration process removed the particles of this size and reduced the concentration of F1.1 to less than 1.07×10^{-5} g cm^{-3}.
(9) Burchard, W.; Kajiwara, K.; Nerger, D.; Stockmayer, W. H. *Macromolecules* **1984**, *17*, 222.
(10) Nemoto, N.; Makita, Y.; Tsunashima, Y.; Kurata, M. *Macromolecules* **1984**, *17*, 425.
(11) Tsunashima, Y.; Nemoto, N. *Macromolecules* **1984**, *17*, 2931. Batchelor, G. R. *J. Fluid Mech.* **1972**, *52*, 245. *Ibid.* **1976**, *74*, 1.
(12) Davidson, N. S.; Fetters, L. J.; Funk, W. G.; Hadjichristidis, N.; Graessley, W. W. *Macromolecules* **1987**, *20*, 2614.
(13) Lindner, J. S.; Wilson, W. W.; Mays, J. W. *Macromolecules* **1988**, *21*, 3304.
(14) (a) Perrin, J. *J. Physik.* **1934**, *5*, 498. (b) Kuhn, W.; Kuhn, H. *Helv. Chim.* **1945**, *28*, 97.
(15) Oono, Y. *Adv. Chem. Phys.* **1985**, *61*, 301 and ref 5.
(16) Kurata, M.; Kimura, T. *J. Polym. Sci., Polym. Phys. Ed.* **1979**, *17*, 2133.
(17) Dondos, A.; Rempp, P.; Benoit, H. *Macromolecules* **1969**, *130*, 233.
(18) (a) Kurata, M.; Tsunashima, Y.; Iwama, M.; Kamada, K. *Polymer Handbook*, 2nd ed.; Brandrup, J.; Immergut, E. H., Eds.; John Wiley and Sons: New York, 1975; pp IV-1. (b) Huglin, M. B. *Polymer Handbook*, 2nd ed.; John Wiley & Sons: New York, 1975; pp IV-267. (c) Rudd, J. F. *Polymer Handbook*, 2nd ed.; John Wiley & Sons: New York, 1975; pp V-59. (d) Stempel, G. H. *Polymer Handbook*, 2nd ed.; John Wiley & Sons: New York, 1975; pp V-1.
(19) The $D(c)$ value for F1.1 was shown by a symbol (○) and was plotted against the nominal concentration (see the text) for convenience sake.
(20) Tsunashima, Y. *Macromolecules*, in press.

(21) As described around eq 4 and 5, we assumed that the data in a limited concentration region could be simply extrapolated to infinite dilution and that the limiting values represent the characteristic conformational properties of the polymers in this region.
(22) Kimura, T.; Kurata, M. *Macromolecules* **1981**, *14*, 1104.
(23) Mandelkern, L.; Flory, P. J. *J. Chem. Phys.* **1952**, *20*, 212. Scheraga, H. A.; Mandelkern, L. *J. Am. Chem. Soc.* **1953**, *175*, 3181.
(24) In the region of concentration similar to region III, Tuzar et al. indicated coexistence of the unimer and the micelles of a SBS triblock copolymer in the mixed selective solvent THF/allyl alcohol: Tuzar, Z.; Petrus, V.; Kratochvil, P. *Makromol. Chem.* **1974**, *175*, 3181. This situation is fairly different from that of our preseent SB diblock/*n*-decane system because the solution corresponding to the filled circle in Figure 12 in region III gave us still near-monodisperse particle sizes.[20] It might be due to the difference in the chain architecture and the solvents used in both systems.
(25) Noolandi, J.; Hong, K. M. *Macromolecules* **1983**, *16*, 1443.
(26) Halperin, A. *Macromolecules* **1987**, *20*, 2943.

Registry No. SB1, 106107-54-4; *n*-decane, 124-18-5.

Swelling Equilibria for Positively Ionized Polyacrylamide Hydrogels

Herbert H. Hooper, John P. Baker, Harvey W. Blanch, and John M. Prausnitz*

Chemical Engineering Department, University of California, and Materials and Chemical Sciences Division, Lawrence Berkeley Laboratory, 1 Cyclotron Road, Berkeley, California 94720. *Received June 6, 1989; Revised Manuscript Received August 4, 1989*

ABSTRACT: Swelling equilibria are reported for polyacrylamide gels in water and for copolymer gels containing acrylamide and [(methacrylamido)propyl]trimethylammonium chloride (MAPTAC) in aqueous NaCl solutions. Gel swelling was investigated as a function of gel structure (cross-link density and monomer concentration), degree of gel ionization (relative amount of charged comonomer) and solution ionic strength. A gel-swelling model is presented which describes polymer/solvent mixing effects using a recently proposed lattice model developed for aqueous/polymer systems; this model accounts for hydrogen bonding in aqueous solutions by distinguishing between different types of contact sites on a solvent molecule or polymer segment. The elastic contribution to swelling is represented using a network theory which accounts for nonaffine displacement of network junctions under strain; polyelectrolyte effects on swelling are described using ideal Donnan theory. Swelling equilibria for uncharged polyacrylamide networks in water are correlated using the gel-swelling model. The model describes reasonably well the effect of cross-link density on swelling but fails to reproduce accurately the dependence of swelling on monomer concentration at preparation. Exchange-energy parameters obtained from polyacrylamide gel-swelling measurements are used to predict swelling in salt solutions for acrylamide/MAPTAC copolymer gels. The model predicts well the effect of gel charge density and solution ionic strength on swelling; however, the effect of monomer concentration is not accurately predicted. Further work is needed to quantify the effect of monomer concentration on the swelling and elastic properties of polyacrylamide hydrogels.

Introduction

Hydrogels have widespread applications in the medical, pharmaceutical, and related fields.[1] In recent years, particular interest has been devoted to gels exhibiting phase transitions (i.e., volume collapse) in response to changes in external conditions. Since the first reported observation of gel collapse,[2] collapse phenomena have been intensely investigated[3] and novel applications have been proposed in a variety of areas, including solute recovery,[4] controlled release,[5] and environmentally sensitive membranes.[6]

A thermodynamic framework has long existed for interpreting gel-swelling equilibria in terms of gel and solution properties;[7] this framework, however, is often unsuitable for hydrogels. Aqueous solutions (e.g., hydrogels) are characterized by strong, orientation-dependent interactions (hydrogen bonds), which can dramatically influence phase (swelling) equilibria. Random-mixing polymer-solution models (e.g., Flory–Huggins theory) do not account for specific interactions and thus often fail to describe correctly phase behavior in aqueous solutions. For example, observed lower critical solution behavior in aqueous poly(*N*-isopropylacrylamide) gels cannot be explained using Flory–Huggins theory unless the Flory interaction parameter is given an unrealistic temperature dependence. This behavior can, however, be explained using a lattice model which accounts for hydrogen bonding by distinguishing between different types of interaction sites.[8]

In addition to polymer/solvent compatibility, gel phase behavior depends on gel structure. Network elasticity theories prescribe relationships between gel structure and gel deformational and swelling properties. Model networks of known structure[9-11] have been investigated to quantify the effects of structure (in particular, molecular weight between cross-links) on elastomer properties. However, for gels prepared in solution the effect on elastic and swelling properties of monomer concentration at preparation is not well understood.[12,13]

Additional complications in describing hydrogel properties arise when fixed charges are incorporated on the polymer network. A small degree of polyelectrolyte character can affect dramatically gel-swelling properties, including the extent of volume collapse and the conditions under

* To whom correspondence should be addressed.

0024-9297/90/2223-1096$02.50/0